Energy &
Environmental
Science

Accepted Manuscript

ROYAL SOCIETY
OF CHEMISTRY

www.rsc.org/ees

Journal Name

COMMUNICATION

Photosystem I-Polyaniline/TiO$_2$ Solid-State Solar Cells: Simple Devices for Biohybrid Solar Energy Conversion

Received 00th January 20xx,
Accepted 00th January 20xx

DOI: 10.1039/x0xx00000x

www.rsc.org/

Evan A. Gizzie,[a†] J. Scott Niezgoda,[a†] Maxwell T. Robinson,[b] Andrew G. Harris,[a] G. Kane Jennings,[b] Sandra J. Rosenthal,[a] and David E. Cliffel[a]

Novel Photosystem I (PSI) based solid-state solar cells were prepared by directly electropolymerizing polyaniline (PAni) in the presence of solubilized PSI on a TiO$_2$ anode. These devices feature a unique bio-derived, photoactive composite layer for efficient charge separation and charge transfer from protein to electrode. This work introduces a new artificial photosynthesis platform for scalable and sustainable solar energy conversion.

The conversion of solar radiation into electricity has been integral in the effort to develop novel alternative energy solutions. Photosynthesis provides a uniquely efficient platform for the development of new solar energy conversion systems and has subsequently spawned a plethora of research strategies to develop bioinspired materials, catalysts, devices, and cell architectures to replicate the efficiency achieved in nature.[1] Alternatively, achievements have been made in directly extracting and utilizing the photoactive proteins that drive photosynthesis. Photosystem I (PSI) is a protein complex that, upon photoexcitation, generates an electron-hole pair with near unity quantum efficiency.[2] Based on this remarkable efficiency and the unidirectional electron transport vector of PSI, it has attracted attention as a biomolecular photodiode to be used in the fabrication of biohybrid photovoltaic electrodes.[3–7]

The development of plant based biohybrid electrodes was pioneered in the 1980's through the successful immobilization of photosynthetic components on electrodes. Agostiano et. al., in 1983, successfully immobilized PSII and PSI on platinum as one of the first examples presenting the viability of a semi-artificial photosynthetic device.[8] Additional pioneering work was achieved by Katz et. al. in which immobilization methods were developed for the covalent attachment and alignment of photosynthetic reaction centers on PtO,[9] and later pyrolytic carbon,[10] for directed electron transport from protein to electrode. In addition to this work, Greenbaum et. al. provided major breakthroughs with the chemical platinization of intact chloroplasts,[11] and later with isolated PSI,[12] for photodriven bio-hydrogen production. Based on these fundamental studies, subsequent decades of research have been dedicated to the creation of artificial photosynthetic devices and biohybrid electrodes as effective bio-derived solar energy conversion platforms.

When incorporated into a traditional biohybrid electrode, photoexcitation of the bound antenna chlorophylls of PSI causes an excited state energy transfer, that results in electron hole pair formation at the "special pair" chlorophyll dimer (denoted as P700) located in the interior of the protein.[13] Following charge dissociation, the excited electron is transported internally through a series of phylloquinone mediators until reaching the terminal [4Fe-4S] iron-sulfur clusters.[14] At the final iron-sulfur cluster, F$_B$, an electron with an energy of -3.9 eV with respect to the vacuum level is accepted by an artificial electrochemical mediator, such as methyl viologen. Concurrent to this process, a hole is transported away from the oxidized P700$^+$ center by an electrode to reduce the special pair and turn over the system for subsequent energy transfer.

In previous generation PSI-based bioelectrodes, protein films were assembled onto metallic substrates in monolayer or multilayer forms acting as a photoactive material for direct photocurrent generation.[15–18] These biohybrid electrodes were able to produce photocurrent densities in the μA cm^{-2} regime when coupled with an appropriate diffusional redox mediator. Through the use of semiconductor electrodes, it has been shown that favorable electron transfer is produced by the alignment between energy bands of a carefully selected semiconductor and PSI. In 2012, both LeBlanc et al.[19] and Mershin et al.,[20] demonstrated this concept by producing PSI-loaded p-doped silicon and ZnO electrodes, respectively. Performance greatly surpassed that which was previously achievable on metallic electrodes in both studies. Recently, hematite has also demonstrated particular utility as a narrow

---

[a] *Department of Chemistry, Vanderbilt University, Nashville, TN 37235-1822*
[b] *Department of Chemical and Biomolecular Engineering, Nashville, TN 37235-1604*

† These authors contributed equally to this work

Electronic Supplementary Information (ESI) available: Experimental details PSI extraction, device fabrication, solar testing, film thickness optimization and photograph of completed device. See DOI: 10.1039/x0xx00000x band gap semiconducting electrode material in pseudo-dye sensitized solar cells with PSI.[21] However, all of these devices have fundamental limitations, specifically the need for liquid diffusional mediators and the cost associated with the fabrication materials.

To alleviate the need for liquid electrolytes, PSI-based solar energy conversion strategies have shifted toward the development of solid-state photovoltaics, and away from wet-cell PSI-based devices. The initial feasibility of solid-state PSI films was demonstrated through the preparation of protein films on gold electrodes that retained photoactivity and electrochemical response under dry conditions.[22,23] In a study by Gordiichuk et al. in 2014, state-of-the-art solid-state biohybrid photovoltaic devices were prepared by assembling a monolayer of cyanobacterial PSI onto a TiO_2 substrate and backing the device with a polytriarylamine hole-conducting layer and MoO_3/Al cathode.[24] Those devices presented a novel breakthrough, but were limited by extensive processing, air sensitivity, and costly materials. To further enhance the performance, sustainability, and scalability of PSI solid-state photovoltaics, we have developed a novel PSI solar cell utilizing a solid polyaniline-PSI composite material as the photosensitizing layer on a TiO_2 semiconductor anode and an evaporated Ag cathode. TiO_2 on FTO-coated glass was selected as the anodic material based on the favorable alignment of its conduction band with the terminal iron-sulfur cluster of PSI (Fig. 1). Based on this energetic alignment, TiO_2 has demonstrated particular utility in previous studies with PSI modified electrodes.[20,25,26] Additionally, the low cost of TiO_2, ease of preparation, and transparency in the visible spectrum make it an ideal electrode material. However, previous PSI-modified TiO_2 electrodes, analogous to dye sensitized solar cells, are limited by the monolayer loading capacity of protein on the substrate.

In this study, PSI was entrapped within an electropolymerized PAni film grown directly on the TiO_2 anode. This film deposition method creates a three-dimensional network of protein enveloped within a conductive matrix with high electron transport kinetics from enzyme to electrode. The photosensitizing PAni-PSI layer was prepared potentiostatically from the electropolymerization of aniline in the presence of solubilized PSI, purified from spinach leaves. The evaporation of a metallic cathode on the PAni-PSI/TiO_2 structure produced a low-cost solid-state photovoltaic device, prepared using facile methods with a bio-derived photoactive layer.

Polyaniline (PAni) has previously been shown to be an exceptional charge transfer material in redox mediated biohybrid cells.[27] For these devices, HCl-doped, emeraldine salt PAni was prepared as the polymeric matrix for the PSI films on TiO_2 due to its high conductivity and ease of preparation.[28] As compared to other conductive polymers, PAni represents the superior material for protein entrapment using electrochemical polymerization. Aniline is water soluble unlike most other organic monomers that are capable of electropolymerization. Additionally, the potential required for electropolymerization is lower than many other comparable organic monomers and analogs, thus reducing the risk of protein and/or substrate degradation. This film preparation method allows the material to act as a solid conductor for electron transport while also providing a three-dimensional network for increased PSI-loading and light adsorption. Active PSI is entrapped in the polyaniline film during

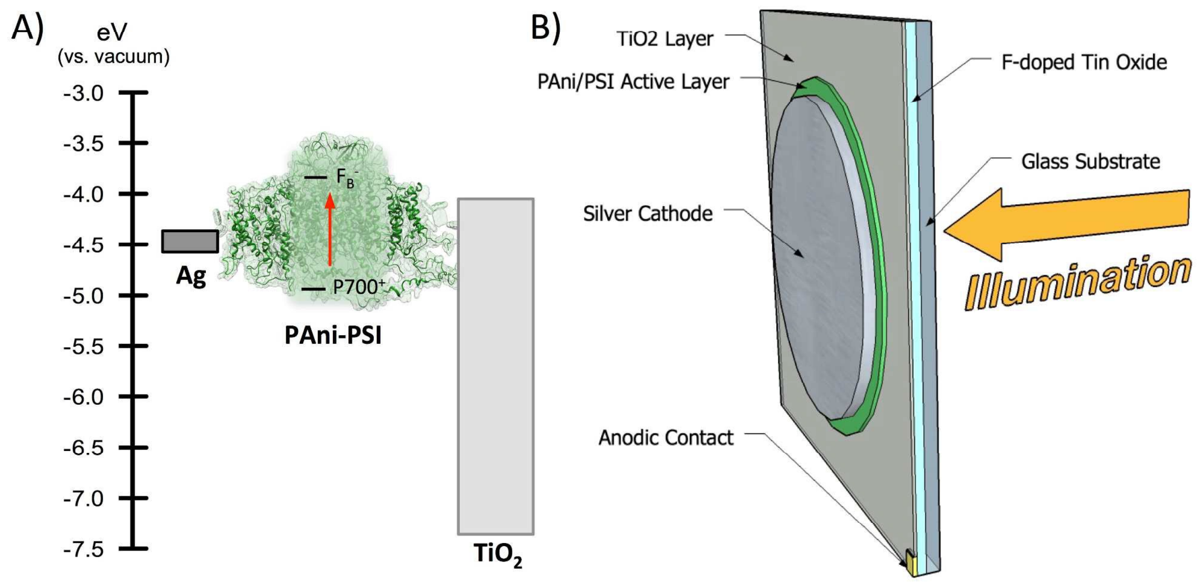

Fig. 1 A) Energy diagram presenting the relationship between the metallic silver cathode, PSI's oxidized $P700^+$ center and reduced iron-sulfur cluster (F_B^-), and the conduction band of the TiO_2 anode. B) Schematic stack-up of the device. The silver cathode layer, PAni-PSI composite layer, and transparent TiO_2 layer on FTO/glass are labelled. Additionally, illumination through the anodic layer is depicted.

electropolymerization as represented by a protein density of approximately 15 nmol cm^{-3} determined previously via ICP-OES.[25] Through growth of the composite PAni-PSI layer on the TiO_2 anode, film thicknesses were controlled by means of electropolymerization time at +6.5 V vs. Ag/AgCl. It was found that films grown for 120 s produced the best performing devices in terms of efficiency (Fig. S1 of ESI†).

The energy diagram presented in Fig. 1 shows the favorable energetic band alignment between the F_B site of PSI and the conduction band of TiO_2. The n-type anatase TiO_2 accepts electrons from the PAni-PSI composite with its conduction band at approximately -4.2 eV.[29] PAni plays a critical role in this device as it shuttles electrons from PSI to the anode through a chain hopping mechanism, introduced by the mixed redox states of emeraldine salt polymer.[30] From the cathodic side of the device, the evaporated silver layer accepts and transports holes away from the oxidized P700$^+$ reaction center of the protein. In Fig. 1B, a layered schematic is presented showing the complete device with silver cathode, PAni-PSI film, and transparent TiO_2 layer on an FTO/glass substrate. Due to the inverted architecture of this device, the PAni-PSI photoactive layer is illuminated through the transparent anode.

Using scanning electron microscopy (SEM) the device cross-section was imaged. Distinct layers were visually identified as the glass, FTO, TiO_2, PAni-PSI, and silver components of the device (Fig. S2 of ESI†). The composition of each device layer was confirmed using EDS elemental mapping (Fig. S3 of the ESI†), thus verifying the solid-state device architecture. The PAni-PSI active layer was approximated to be 350 nm for the layer prepared from 120 s of potentiostatic polymerization. A PAni-PSI composite layer of this thickness presumably reaches an optimum interplay between high optical density for maximum photon absorption while being thin enough to allow for efficient carrier diffusion in the film. Often observed in polymer-semiconductor devices with inverted architecture (similar to this device), a thick polymer active layer increases the hopping distance for holes to reach the cathode, thus diminishing photocurrent density and efficiency as the film thickness increases.[31]

The Ag/PAni-PSI/TiO_2 solid-state devices were evaluated under solar simulation conditions. I-V curves for typical devices are shown in Fig 2. For the PAni-PSI devices, typical short circuit current densities (J_{SC}) of 72 μA cm^{-2} were observed. This average photocurrent density surpasses the previous state-of-the-art solid-state PSI photovoltaic device by nearly 250-fold.[24] In addition to the large photocurrent densities, the use of silver cathodes consistently produces open-circuit voltages (V_{OC}) of approximately 300 mV. As expected, the PAni-only devices (shown in blue) performed poorly, relative to the PSI-loaded devices. The photocurrent densities, open circuit potentials, and efficiencies of the PAni-only control devices were approximately 3-fold smaller than the PAni-PSI devices. Table 1 summarizes the performance metrics of J_{SC}, V_{OC}, fill factor, and external quantum efficiency (EQE) for the Ag/PAni-PSI/TiO_2 and Ag/PAni-only/TiO_2 devices. Action spectra relating the illumination wavelength to quantum efficiency were collected for PAni-PSI and PAni-only solid-state devices (shown in Fig. S4 of the ESI†). As expected, the quantum efficiency of the PSI-loaded device correlates directly with the absorption spectrum of PSI's chlorophyll antenna, and thus indicates PSI's role in charge separation in these solid-state devices.

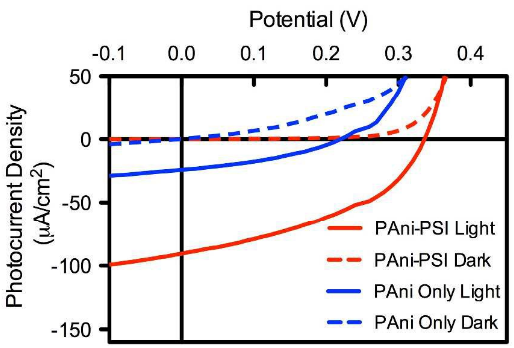

Fig. 2 I-V curves for Ag/PAni-PSI/TiO_2 and Ag/PAni-only/TiO_2 solid-state devices tested in the dark and under AM1.5 solar

To better corroborate the band alignment predictions of this novel PSI-composite solid-state device, the metallic cathode material was altered. With all other components of the device kept constant, devices were prepared with an evaporated metal of lower or higher work function than silver. It was hypothesized that gold, with a work function of -5.1 eV, would perform poorly as a cathodic material because it is energetically lower than the P700/P700$^+$ redox site of PSI, thus making it unable to accept holes from the oxidized protein. An evaporated aluminum cathode should produce significantly less photocurrent than silver because the work function of Al (-4.08 eV) is higher than the conduction band of TiO_2. This energetic mismatch will favor electron-hole pair recombination in the PAni matrix, over the effective charge separation and migration pathway through the entrapped PSI. The comparison of silver, gold, and aluminum as cathode materials in PAni-PSI/TiO_2 devices is presented in Fig. 3. As predicted, the use of silver as the cathode material resulted in

Table 1 Performance of PAni-PSI devices and PAni-only devices. For each value, the average and standard error are reported.

Active Layer Type	Current Density, J_{SC} (μA cm^{-2})	Open Circuit Potential, V_{OC} (V)	Fill Factor	External Quantum Efficiency (%)
PAni-PSI (n = 13)	72 ± 3	0.299 ± 0.004	0.420 ± 0.007	0.0091 ± 0.0006
PAni-only (n = 16)	21 ± 7	0.100 ± 0.003	0.19 ± 0.05	0.0022 ± 0.0009

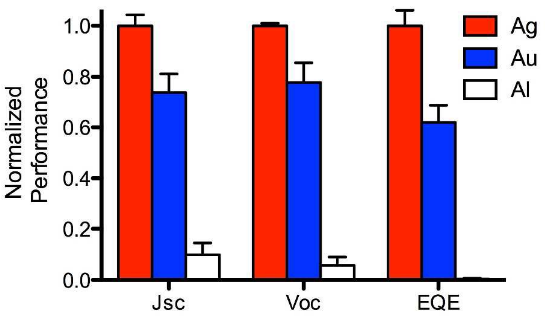

Fig. 3 Performance of Ag, Au, and Al as evaporated cathodes in PAni-PSI/TiO_2 solid-state devices. For clarity, each metric was normalized to the highest performing electrode material. Error bars represent the standard error of a minimum of 4 replicates.

the highest photocurrents, open-circuit voltages, and efficiencies based on its favorable energy alignment with PSI and TiO_2.

In addition to the performance of this solid-state biophotovoltaic, there are superior advantages over previous PSI devices in cost and long-term stability. The utility of Ag/PAni-PSI/TiO_2 devices has been demonstrated here by the simple design, wide availability of PSI from spinach and other plants,[32] and low-cost device fabrication. More importantly, the stability of this device for long-term performance under real world conditions has proven great utility. By codepositing PAni and PSI, the conductive polymer advantageously serves as a stabilizing matrix for the entrapped PSI. Operational stability is demonstrated in Fig. 4 where the performance of Ag/PAni-PSI/TiO_2 devices was monitored over the course of three days with 12-hour periods of light and dark. This light cycling was intended to mimic the solar cycle found in Nature.

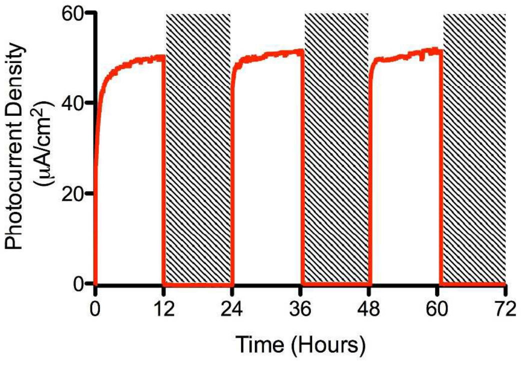

Fig. 4 Performance of a typical Ag/PAni-PSI/TiO_2 device under 12-hour cycles of light and dark for three days. Shaded gray bars represent the periods in which the sample was not illuminated.

In this three-day study, the photocurrent output did not decline between the 12-hour illumination periods nor intraday for the duration of the study. This indicates the viability of PSI-based solid-state devices in real world settings.

Additionally, the long term storage stability of Ag/PAni-PSI/TiO_2 devices was evaluated by sampling power curves daily over the course of 20 days and stored under open-air conditions at approximately 20 °C, when not in use. These devices retained greater than 85% of original photocurrent output over the course of the 20 days (Fig. S5 of the ESI†), which effectively demonstrates the robustness of the PAni-PSI film as an active layer in solid-state solar energy conversion devices, and presents the feasibility of further development of bio-derived solid-state photovoltaics from low-cost materials.

Conclusions

Using facile and low-cost preparation methods, the photosynthetic protein, PSI, has been successfully incorporated into a conductive polyaniline network for direct photocurrent generation. Through electrochemical polymerization, this organic, bio-derived active layer was grown directly off of transparent TiO_2 electrodes. These photoactive electrodes were then completed with the evaporated metallic cathodes to yield stand-alone solid-state photovoltaics. Solar-simulated I-V analysis revealed that these devices yielded average photocurrent densities of 72 μA cm^{-2}, with an approximate open-circuit voltage of 300 mV, and an external quantum efficiency of 0.01%. This performance greatly exceeds the current state-of-the-art in PSI-derived solid-state photovoltaics by nearly 250-fold in photocurrent output, while also being lower in cost and more stable than previous PSI devices. The novel PAni-PSI/TiO_2 devices represent a major advancement in the field of biohybrid solar energy conversion based on their performance, simple cell design, low-cost fabrication materials, facile preparation methods, and operational longevity.

Acknowledgements

We gratefully acknowledge support from NSF EPSCoR (EPS 1004083), NSF (DMR 1507505), the Scialog Program from the Research Corporation for Science Advancement, and the U.S. Department of Agriculture (2013-67021-21029 USDA). E.A.G. was supported by the Vanderbilt University Mitchum E. Warren Fellowship and the Frederick LeRoy Conover Graduate Research Fellowship. Additionally, we acknowledge the Vanderbilt Institute of Nanoscale Science and Engineering (VINSE) for use of clean room facilities and imaging core, as well as Will Erwin of the Bardhan Research Group for providing a tunable laser source for IPCE experiments. We also acknowledge Shellie Richards for assistance in preparation of this manuscript.

References

1 A. A. Boghossian, M. H. Ham, J. H. Choi and M. S. Strano, *Energy Environ. Sci.*, 2011, **4**, 3834–3843.

2 S. W. Hogewoning, E. Wientjes, P. Douwstra, G. Trouwborst, W. van Ieperen, R. Croce and J. Harbinson, *Plant Cell*, 2012, **24**, 1921–1935.

3 G. LeBlanc, E. A. Gizzie, S. Yang, D. E. Cliffel and G. K. Jennings, *Langmuir*, 2014, **30**, 10990–11001.

4 A. Badura, T. Kothe, W. Schuhmann and M. Rogner, *Energy Environ. Sci.*, 2011, **4**, 3263–3274.

5 J. Kargul, J. D. Janna Olmos and T. Krupnik, *J. Plant Physiol.*, 2012, **169**, 1639–1653.

6 O. Yehezkeli, R. Tel-Vered, D. Michaeli, I. Willner and R. Nechushtai, *Photosynth Res*, 2013.

7 L. Nagy, M. Magyar, T. Szabó, K. Hajdu, L. Giotta, M. Dorogi and F. Milano, *Curr. Protein Pept. Sci.*, 2014, **15**, 363.

8 A. Agostiano, A. Ceglie, M. Della Monica, C. Studi and V. Amendola, *Bioelectrochemistry Bioenerg.*, 1983, **10**, 377–384.

9 E. Y. Katz, A. Y. Shkuropatov, O. I. Vagabova and V. A. Shuvalov, *Biochim. Biophys. Acta - Bioenerg.*, 1989, **976**, 121–128.

10 E. Katz, *J. Electroanal. Chem.*, 1994, **365**, 157–164.

11 E. Greenbaum, *Science (80-.).*, 1985, **230**, 1373–1375.

12 J. W. Lee, I. Lee, P. D. Laible, T. G. Owens and E. Greenbaum, *Biophys. J.*, 1995, **69**, 652–659.

13 K. Brettel, *Biochim. Biophys. Acta*, 1997, **1318**, 322–373.

14 K. Brettel and W. Leibl, *Biochim. Biophys. Acta*, 2001, **1507**, 100–114.

15 P. N. Ciesielski, C. J. Faulkner, M. T. Irwin, J. M. Gregory, N. H. Tolk, D. E. Cliffel and G. K. Jennings, *Adv. Funct. Mater.*, 2010, **20**, 4048–4054.

16 D. Mukherjee, M. May, M. Vaughn, B. D. Bruce and B. Khomami, *Langmuir*, 2010, **26**, 16048–16054.

17 A. K. Manocchi, D. R. Baker, S. S. Pendley, K. Nguyen, M. M. Hurley, B. D. Bruce, J. J. Sumner and C. A. Lundgren, *Langmuir*, 2013, **29**, 2412–2419.

18 B. S. Ko, B. Babcock, G. K. Jennings, S. G. Tilden, R. R. Peterson, D. Cliffel and E. Greenbaum, *Langmuir*, 2004, **20**, 4033–4038.

19 G. LeBlanc, G. Chen, E. A. Gizzie, G. K. Jennings and D. E. Cliffel, *Adv. Mater.*, 2012, **24**, 5959–5962.

20 A. Mershin, K. Matsumoto, L. Kaiser, D. Yu, M. Vaughn, M. K. Nazeeruddin, B. D. Bruce, M. Graetzel and S. Zhang, *Sci. Rep.*, 2012, **2**.

21 K. Ocakoglu, T. Krupnik, B. van den Bosch, E. Harputlu, M. P. Gullo, J. D. J. Olmos, S. Yildirimcan, R. K. Gupta, F. Yakuphanoglu, A. Barbieri, J. N. H. Reek and J. Kargul, *Adv. Funct. Mater.*, 2014, **24**, 7467–7477.

22 I. Carmeli, L. Frolov, C. Carmeli and S. Richter, *J. Am. Chem. Soc.*, 2007, **129**, 12352–12353.

23 R. Das, P. J. Kiley, M. Segal, J. Norville, A. A. Yu, L. Y. Wang, S. A. Trammell, L. E. Reddick, R. Kumar, F. Stellacci, N. Lebedev, J. Schnur, B. D. Bruce, S. G. Zhang and M. Baldo, *Nano Lett.*, 2004, **4**, 1079–1083.

24 P. I. Gordiichuk, G. A. H. Wetzelaer, D. Rimmerman, A. Gruszka, J. W. De Vries, M. Saller, D. a. Gautier, S. Catarci, D. Pesce, S. Richter, P. W. M. Blom and A. Herrmann, *Adv. Mater.*, 2014, **26**, 4863–4869.

25 V. B. Shah, W. R. Henson, T. S. Chadha, G. Lakin, H. Liu, R. E. Blankenship and P. Biswas, *Langmuir*, 2015, **31**, 1675–1682.

26 D. Yu, M. Wang, G. Zhu, B. Ge, S. Liu and F. Huang, *Sci. Rep.*, 2015, **5**, 9375.

27 E. A. Gizzie, G. LeBlanc, G. K. Jennings and D. E. Cliffel, *ACS Appl. Mater. Interfaces*, 2015, **7**, 9328–9335.

28 K. M. Molapo, P. M. Ndangili, R. F. Ajayi, G. Mbambisa, S. M. Mailu, N. Njomo, M. Masikini, P. Baker and E. I. Iwuoha, *Int. J. Electrochem. Sci.*, 2012, **7**, 11859–11875.

29 M. Grätzel, *Nature*, 2001, **414**, 338–344.

30 M. Baćani, M. Novak, I. Kokanović and D. Babić, *Synth. Met.*, 2013, **172**, 28–31.

31 T. Xu and Q. Qiao, *Energy Environ. Sci.*, 2011, **4**, 2700–2720.

32 D. Gunther, G. LeBlanc, D. E. Cliffel and G. K. Jennings, *Ind. Biotechnol.*, 2013, **9**, 37–41.

Photosystem I-Polyaniline/TiO_2 Solid-State Solar Cells: Simple Devices for Biohybrid Solar Energy Conversion

Evan A. Gizzie, J. Scott Niezgoda, G. Kane Jennings, Sandra J. Rosenthal, and David E. Cliffel*

Table of Contents Entry:

Novel biophotovoltaic devices were prepared by electrochemically entrapping Photosystem I in a conductive polyaniline film, grown *in situ* on TiO_2 anodes**.**

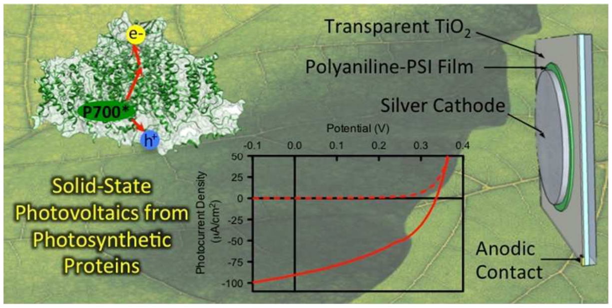

Photosystem I-Polyaniline/TiO_2 Solid-State Solar Cells: Simple Devices for Biohybrid Solar Energy Conversion

Evan A. Gizzie, J. Scott Niezgoda, G. Kane Jennings, Sandra J. Rosenthal, and David E. Cliffel*

Broader context

Photosynthesis provides a unique model by which solar energy is harvested and converted into other usable forms. For this reason, decades of research have been dedicated to mimicking the solar energy conversion pathways of green plants and autotrophic bacteria, including the direct use of extracted photosynthetic proteins to create photoactive biohybrid electrodes. In this work, the photosynthetic protein, Photosystem I (PSI), was extracted from spinach leaves and used to prepare novel bio-based solid-state solar cells. Previous PSI-based devices have been limited by prohibitive costs, extensive processing, marginal performance, and poor environmental stability. The devices presented here exceed in all of the aforementioned categories through the use of a unique conductive polymer-PSI composite active layer, prepared electrochemically, which acts as a bio-derived photosensitizing layer for direct solar energy conversion. This innovative work introduces a new generation of low-cost, stable, and scalable solid-state biophotovoltaics and bio-derived artificial photosynthetic systems.